Electronic Journal of Differential Equations, Vol. 2026 (2026), No. 91, pp. 1–20.
ISSN: 1072-6691. URL: https://ejde.math.txstate.edu, DOI: 10.58997/ejde.2026.91

GLOBAL DYNAMICS OF TWO SUBCLASSES OF COPPEL'S QUADRATIC SYSTEMS

MAN JIA

Abstract. In this article, we investigate two subclasses of Coppel's planar quadratic differential systems, corresponding to particular forms of Ye's Classes II and III. For the Class II subclass and a subfamily of the Class III subclass, we determine the number of limit cycles and establish complete bifurcation diagrams and global phase portraits in the Poincaré disc. For the remaining cases, we provide a classification of the equilibria and a detailed analysis of their local bifurcations. Furthermore, our results may contribute to a particular understanding of certain dynamical phenomena arising in the shear flows of non-Newtonian fluids.

1. Introduction

In the class of planar polynomial vector fields, quadratic differential systems are the simplest nonlinear systems beyond the linear case. Despite their low algebraic degree, they exhibit remarkably rich global dynamics, involving finite and infinite equilibria, separatrix configurations, limit cycles, and global bifurcations; see, for example, [1, 3, 4, 7, 8, 11, 12, 13, 17, 30, 32, 34, 37, 38]. Quadratic differential systems have consequently received extensive attention in the literature; see, among many others, [2, 6, 10, 25, 26, 27, 28, 29, 31, 35] and the references therein. A landmark achievement was made in 1979, when Shi [33] and, independently, Chen and Wang [5] constructed quadratic differential systems with four limit cycles. Nevertheless, determining the maximum number of limit cycles that a quadratic differential system can possess remains a fundamental open problem. This question is part of the second part of Hilbert's sixteenth problem, which asks for the maximum number of limit cycles of a planar polynomial differential system of degree n and their possible relative positions; see [15, 16, 19, 20].

An important motivation for investigating certain classes of planar quadratic systems arises from the study of shear flows of highly elastic non-Newtonian fluids. In this context, Malkus, Nohel, and Plohr developed finite-dimensional dynamical models arising from the analysis of transient shear flows of non-Newtonian fluids. These models are related to constitutive descriptions of highly elastic liquids and lead to phase-plane problems exhibiting phenomena of particular interest in fluid dynamics [22, 23, 24]. Motivated by a question posed by Nohel concerning the nonexistence of periodic orbits in a specific quadratic system modeling shear flow between parallel plates, Coppel introduced a distinguished class of planar quadratic systems in [9]. The defining feature of this class is a particular factorization structure of the homogeneous quadratic terms. More precisely, Coppel considered systems of the form

$$\begin{aligned} \dot{x} &= P(x,y) = \sum_{j+k=0}^{2} a_{jk} x^j y^k, \\ \dot{y} &= Q(x,y) = \sum_{j+k=0}^{2} b_{jk} x^j y^k, \end{aligned} \tag{1.1}$$

2020 *Mathematics Subject Classification.* 34C07, 34C23, 34A34.
Key words and phrases. Global dynamics; quadratic differential system; global phase; portraits; bifurcation diagram.
©2026. This work is licensed under a CC BY 4.0 license.
Submitted January 18, 2026. Published November 18, 2026.

where P and Q are relatively prime real polynomials of degree at most two, are not both linear, and j, k are nonnegative integers. Furthermore, their homogeneous quadratic parts satisfy

$$\begin{aligned} P_2(x,y) &= (Ax+By)(Dx+Ey), \\ Q_2(x,y) &= (Cx-Ay)(Dx+Ey), \end{aligned} \tag{$*$}$$

where P_2 and Q_2 denote the homogeneous quadratic parts of P and Q, respectively, and $A, B, C, D, E \in \mathbb{R}$. Thus, the two quadratic parts share a common linear factor, while the coefficient matrix of the remaining linear factors has zero trace.

Coppel [9] showed that every system (1.1) satisfying $(*)$ can be reduced to the form

$$\dot{x} = dx - y + mxy + ny^2, \quad \dot{y} = x + hxy - my^2, \tag{1.2}$$

and, through the linear transformation $\bar{x} = -y$, $\bar{y} = x - dy$, to the equivalent form

$$\dot{\bar{x}} = \bar{d}\bar{x} - \bar{y} + \bar{m}\bar{x}^2 + \bar{h}\bar{x}\bar{y}, \quad \dot{\bar{y}} = \bar{x} + \bar{n}\bar{x}^2 - \bar{m}\bar{x}\bar{y}, \tag{1.3}$$

where

$$\bar{d} = d, \quad \bar{h} = h, \quad \bar{m} = m - hd, \quad \bar{n} = n + 2dm - hd^2.$$

All the parameters $d, \bar{d}, h, \bar{h}, m, \bar{m}, n, \bar{n}$ are real. For simplicity, we shall henceforth write x and y in place of $\bar{x}$ and $\bar{y}$ in system (1.3).

Systems in Coppel's class have at most three equilibria at infinity. In [9], Coppel established that any quadratic system satisfying $(*)$ and having at most two equilibria at infinity possesses at most one limit cycle. For the remaining case, in which there are three equilibria at infinity, he conjectured that every such system has at most two limit cycles. His result can be stated as follows.

Theorem 1.1 ([9, Theorem 1]). *If a quadratic system* (1.1) *satisfies condition* $(*)$ *and has at most two equilibria at infinity, then either it has a center or it has at most one periodic orbit. Moreover, if a unique periodic orbit exists, then it is a limit cycle with a nonzero characteristic exponent.*

In this article, we focus on system (1.3), which is precisely the canonical form introduced by Ye [35]. Ye established that a necessary condition for a quadratic system to possess a closed orbit is that it be transformable into one of the following three canonical classes: Class I:

$$\begin{aligned} \dot{x} &= -y + \delta x + lx^2 + \alpha xy + \beta y^2, \\ \dot{y} &= x, \end{aligned} \tag{1.4}$$

class II:

$$\begin{aligned} \dot{x} &= -y + \delta x + lx^2 + \alpha xy + \beta y^2, \\ \dot{y} &= x(1+\xi x), \quad \xi \neq 0, \end{aligned} \tag{1.5}$$

and Class III:

$$\begin{aligned} \dot{x} &= -y + \delta x + lx^2 + \alpha xy + \beta y^2, \\ \dot{y} &= x(1+\xi x + \eta y), \quad \eta \neq 0. \end{aligned} \tag{1.6}$$

Here $\delta, l, \alpha, \beta, \xi, \eta \in \mathbb{R}$.

We now distinguish three parameter regimes of system (1.3), according to whether $\bar{m}$ and $\bar{n}$ vanish.

If $\bar{m} = \bar{n} = 0$, system (1.3) reduces to

$$\dot{x} = \bar{d}x - y + \bar{h}xy, \quad \dot{y} = x. \tag{1.7}$$

This is a special case of Ye's Class I, with $\delta = \bar{d}$, $l = \beta = 0$, and $\alpha = \bar{h}$. It follows from [35, Theorem 12.5 p. 269] that system (1.7) has a global center when $\bar{d} = 0$, whereas it has neither closed orbits nor singular closed orbits when $\bar{d} \neq 0$. The global phase portraits of system (1.7) in the Poincaré disc can be found in [1, 21].

If $\bar{m} = 0$ and $\bar{n} \neq 0$, system (1.3) becomes

$$\dot{x} = \bar{d}x - y + \bar{h}xy, \quad \dot{y} = x + \bar{n}x^2. \tag{1.8}$$

Applying the scaling transformation

$$(x, y) \mapsto \left(\frac{x}{\bar{n}}, \frac{y}{\bar{n}}\right),$$

we obtain the equivalent system

$$\dot{x} = \mu_1 x - y + \mu_2 xy, \quad \dot{y} = x + x^2, \tag{1.9}$$

which is a special case of Ye's Class II, with $\delta = \mu_1$, $l = \beta = 0$, $\alpha = \mu_2$, and $\xi = 1$, where

$$\mu_1 = \bar{d}, \quad \mu_2 = \frac{\bar{h}}{\bar{n}}.$$

Moreover, system (1.9) is invariant under the parameter transformation

$$(y, t, \mu_1) \mapsto (-y, -t, -\mu_1).$$

Consequently, it suffices to consider $\mu_1 \geq 0$.

Finally, suppose that $\bar{m} \neq 0$. Under the scaling transformation

$$(x, y) \mapsto \left(\frac{x}{\bar{m}}, \frac{y}{\bar{m}}\right),$$

system (1.3) is transformed into

$$\dot{x} = ax - y + x^2 + bxy, \quad \dot{y} = x + cx^2 - xy, \tag{1.10}$$

where

$$a = \bar{d}, \quad b = \frac{\bar{h}}{\bar{m}}, \quad c = \frac{\bar{n}}{\bar{m}}.$$

This is a special case of Ye's Class III, corresponding to $\delta = a$, $l = 1$, $\alpha = b$, $\beta = 0$, $\xi = c$, and $\eta = -1$. Notice that system (1.10) is invariant under the transformation

$$(x, t, a, b, c) \mapsto (-x, -t, -a, -b, -c). \tag{1.11}$$

Hence, without loss of generality, we may restrict our attention to the case $c \geq 0$.

The main objective of this paper is to investigate the global dynamics of system (1.9) and system (1.10) in the case $c = 0$, with particular emphasis on their limit cycles, singular closed orbits, and global phase portraits in the Poincaré disc. When $c > 0$, the equilibrium configurations of system (1.10) become more intricate, making a complete global analysis substantially more involved. In this case, we classify the equilibria and investigate their local bifurcations, leaving the complete global analysis for future work.

The remainder of the paper is organized as follows. Section 2 presents the complete bifurcation diagrams and global phase portraits of system (1.9) and system (1.10) with $c = 0$, together with the local bifurcation sets of system (1.10) for $c > 0$. Section 3 contains the proofs of the main results.

2. Main results

Theorem 2.1. *For any $(\mu_1, \mu_2) \in [0, +\infty) \times \mathbb{R}$, the bifurcation diagram of system (1.9) consists of the following bifurcation curves:*

(i) *there is a pitchfork bifurcation curve at infinity*

$$P := \{(\mu_1, \mu_2) \in [0, +\infty) \times \mathbb{R} : \mu_2 = 0\};$$

(ii) *there is a degenerate equilibrium bifurcation curve at infinity*

$$DE_1 := \{(\mu_1, \mu_2) \in [0, +\infty) \times \mathbb{R} : \mu_2 = -1\}.$$

Moreover, the corresponding global phase portraits in the Poincaré disc of system (1.9) are shown in Figure 1, where

$$\begin{aligned}
R_1 &:= \{(\mu_1, \mu_2) \in [0, +\infty) \times \mathbb{R} : \mu_1 > 0,\ \mu_2 > 0\},\\
R_2 &:= \{(\mu_1, \mu_2) \in [0, +\infty) \times \mathbb{R} : \mu_1 = 0,\ \mu_2 > 0\},\\
R_3 &:= \{(\mu_1, \mu_2) \in [0, +\infty) \times \mathbb{R} : \mu_1 > 0,\ -1 < \mu_2 < 0\},\\
R_4 &:= \{(\mu_1, \mu_2) \in [0, +\infty) \times \mathbb{R} : \mu_1 = 0,\ -1 < \mu_2 < 0\},
\end{aligned}$$

$$
\begin{aligned}
R_5 &:= \{(\mu_1,\mu_2) \in [0,+\infty)\times\mathbb{R} : \mu_1 > 0,\ \mu_2 < -1\},\\
R_6 &:= \{(\mu_1,\mu_2) \in [0,+\infty)\times\mathbb{R} : \mu_1 = 0,\ \mu_2 < -1\},\\
P_1 &:= \{(\mu_1,\mu_2) \in [0,+\infty)\times\mathbb{R} : \mu_1 > 0,\ \mu_2 = 0\},\\
P_2 &:= \{(\mu_1,\mu_2) \in [0,+\infty)\times\mathbb{R} : \mu_1 = 0,\ \mu_2 = 0\},\\
DE_{11} &:= \{(\mu_1,\mu_2) \in [0,+\infty)\times\mathbb{R} : \mu_1 > 0,\ \mu_2 = -1\},\\
DE_{12} &:= \{(\mu_1,\mu_2) \in [0,+\infty)\times\mathbb{R} : \mu_1 = 0,\ \mu_2 = -1\}.
\end{aligned}
$$

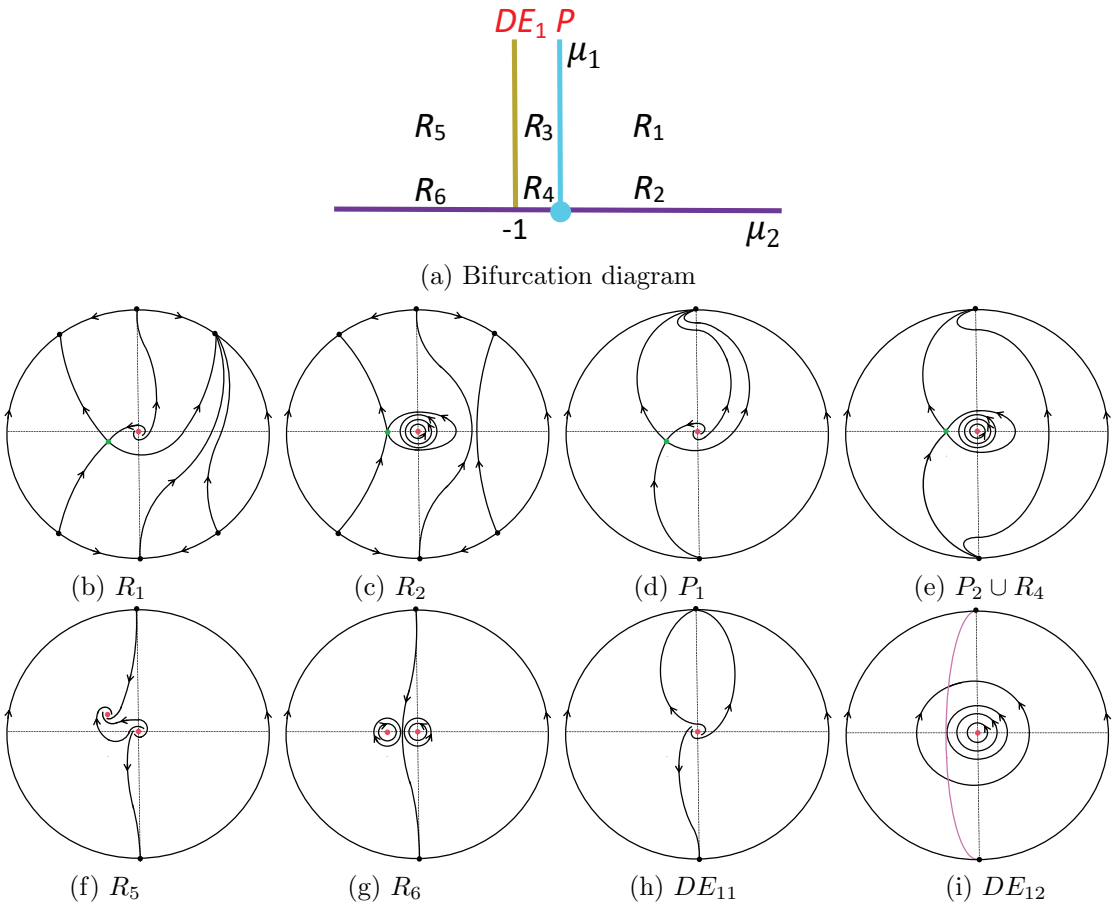

(a) Bifurcation diagram

(b) R_1 (c) R_2 (d) P_1 (e) $P_2 \cup R_4$

(f) R_5 (g) R_6 (h) DE_{11} (i) DE_{12}

FIGURE 1. Complete bifurcation diagram and global phase portraits in the Poincaré disc of system (1.9) with $(\mu_1,\mu_2) \in [0,+\infty)\times\mathbb{R}$

Theorem 2.2. *For each $(a,b,c) \in \mathbb{R}^2 \times \{0\}$, the bifurcation diagram of system (1.10) consists of the following bifurcation curves:*

(i) *there is a Hopf bifurcation curve at E_0*

$$H_1 := \{(a,b,c) \in \mathbb{R}^2 \times \{0\} : a = 0,\ b \neq 0\};$$

(ii) *there is a degenerate equilibrium bifurcation curve at infinity*

$$DE_2 := \{(a,b,c) \in \mathbb{R}^2 \times \{0\} : b = 0\};$$

(iii) *there is a heteroclinic bifurcation curve*

$$HE_1 := \{(a,b,c) \in \mathbb{R}^2 \times \{0\} : a = \varphi(b)\},$$

where $\varphi(0) = 0$, and $-2 < \varphi(b) < 2$ for $b \neq 0$.

In this case, system (1.10) *admits one limit cycle in* S_2 *and* S_5*, and the corresponding global phase portraits in the Poincaré disc of system* (1.10) *are shown in Figure 2, where*

$$\begin{aligned}
S_1 &:= \{(a,b,c) \in \mathbb{R}^2 \times \{0\} : a > 0,\ b > 0\},\\
S_2 &:= \{(a,b,c) \in \mathbb{R}^2 \times \{0\} : \varphi(b) < a < 0,\ b > 0\},\\
S_3 &:= \{(a,b,c) \in \mathbb{R}^2 \times \{0\} : a < \varphi(b),\ b > 0\},\\
S_4 &:= \{(a,b,c) \in \mathbb{R}^2 \times \{0\} : a < 0,\ b < 0\},\\
S_5 &:= \{(a,b,c) \in \mathbb{R}^2 \times \{0\} : 0 < a < \varphi(b),\ b < 0\},\\
S_6 &:= \{(a,b,c) \in \mathbb{R}^2 \times \{0\} : a > \varphi(b),\ b < 0\},\\
H_{11} &:= \{(a,b,c) \in \mathbb{R}^2 \times \{0\} : a = 0,\ b > 0\};\\
H_{12} &:= \{(a,b,c) \in \mathbb{R}^2 \times \{0\} : a = 0,\ b < 0\},\\
DE_{21} &:= \{(a,b,c) \in \mathbb{R}^2 \times \{0\} : a > 0,\ b = 0\},\\
DE_{22} &:= \{(a,b,c) \in \mathbb{R}^2 \times \{0\} : a = 0,\ b = 0\},\\
DE_{23} &:= \{(a,b,c) \in \mathbb{R}^2 \times \{0\} : a < 0,\ b = 0\},\\
HE_{11} &:= \{(a,b,c) \in \mathbb{R}^2 \times \{0\} : a = \varphi(b),\ b > 0\},\\
HE_{12} &:= \{(a,b,c) \in \mathbb{R}^2 \times \{0\} : a = \varphi(b),\ b = 0\},\\
HE_{13} &:= \{(a,b,c) \in \mathbb{R}^2 \times \{0\} : a = \varphi(b),\ b < 0\}.
\end{aligned}$$

Theorem 2.3. *For each* $(a,b,c) \in \mathbb{R}^2 \times (0,+\infty)$*, system* (1.10) *has the following local bifurcation sets:*

(i) *there is a Hopf bifurcation surface at* E_0*,*

$$H_2 := \{(a,b,c) \in \mathbb{R}^2 \times (0,+\infty) : a = 0,\ b \neq c\}$$

and another Hopf bifurcation surface at E_1*,*

$$H_3 := \big\{(a,b,c) \in \mathbb{R}^2 \times (0,+\infty) : a = \frac{1}{c},\ b < -c - \frac{1}{c}\big\};$$

(ii) *there is a Bautin bifurcation curve at* E_0*,*

$$B := \{(a,b,c) \in \mathbb{R}^2 \times (0,+\infty) : a = 0,\ b = c > 0\};$$

(iii) *there is a saddle-node bifurcation surface*

$$SN := \big\{(a,b,c) \in \mathbb{R}^2 \times (0,+\infty) : bc < -1,\ \Delta = 0,\ a+b+c \neq 0\big\}$$

with $\Delta := (a+b-c)^2 + 4(1+bc)$*;*

(iv) *there is a Bogdanov-Takens bifurcation curve at* E_{12}*,*

$$BT := \big\{(a,b,c) \in \mathbb{R}^2 \times (0,+\infty) : a = \frac{1}{c},\ b = -c - \frac{1}{c}\big\}.$$

3. Proofs of main results

3.1. **Equilibria of system** (1.9)**.** We start by considering the qualitative properties of equilibria of system (1.9).

Lemma 3.1. *For any* $(\mu_1,\mu_2) \in [0,+\infty) \times \mathbb{R}$*, equilibria* $O(0,0), E(-1, -\mu_1/(1+\mu_2))$ *of system* (1.9) *and their qualitative properties are given in Table 1.*

Proof. Clearly, when $\mu_1 \geq 0$, system (1.9) has a unique equilibrium O as $\mu_2 = -1$, and two equilibria O and E as $\mu_2 \neq -1$, see Table 1. Additionally, system (1.9) has one singular line $x = -1$ as $\mu_2 = -1$ and $\mu_1 = 0$.

The Jacobian matrix J_O of system (1.9) at O satisfies $\det J_O = 1$ and $\operatorname{tr} J_O = \mu_1$. Hence, O is a source for $\mu_1 > 0$. For $\mu_1 = 0$, O is a center because system (1.9) is invariant under the transformation $(y,t) \to (-y,-t)$. Thus, the qualitative properties of O are completely classified.

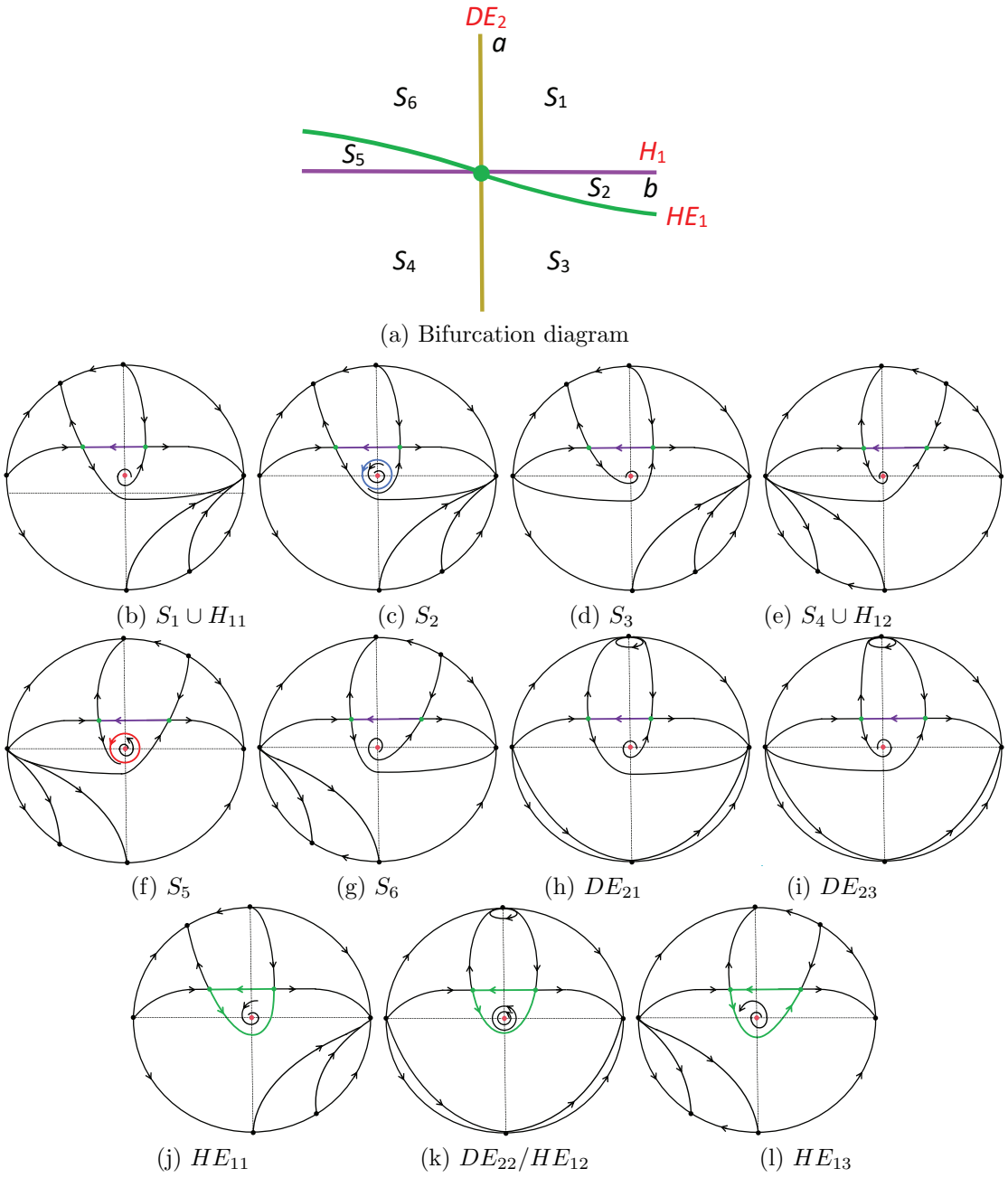

(a) Bifurcation diagram

(b) $S_1 \cup H_{11}$ (c) S_2 (d) S_3 (e) $S_4 \cup H_{12}$

(f) S_5 (g) S_6 (h) DE_{21} (i) DE_{23}

(j) HE_{11} (k) DE_{22}/HE_{12} (l) HE_{13}

FIGURE 2. Bifurcation diagrams and global phase portraits in the Poincaré disc of system (1.10) with $(a, b, c) \in \mathbb{R}^2 \times \{0\}$

Significantly, E exists if and only if $\mu_2 \neq -1$. The Jacobian matrix J_E of system (1.9) at E satisfies $\det J_E = -1 - \mu_2$ and $\operatorname{tr} J_E = \mu_1/(1+\mu_2)$. Hence, E is a saddle for $\mu_2 > -1$. For $\mu_2 < -1$, E is a sink as $\mu_1 > 0$. Additionally, for $\mu_2 < -1$ and $\mu_1 = 0$, E is a center because the phase portrait of system (1.9) is symmetric about the x-axis. Thus, the qualitative properties of E are completely classified. □

Now, we discuss the qualitative properties of equilibria at infinity of system (1.9).

TABLE 1. Numberic and qualitative properties of equilibria of system (1.9)

$(\mu_1,\mu_2)\in[0,+\infty)\times\mathbb{R}$		Equilibria	Type and Stability	
$\mu_2>-1$	$\mu_1>0$	O,E	O: source	E: saddle
	$\mu_1=0$		O: center	
$\mu_2=-1$	$\mu_1>0$	O	O: source	
	$\mu_1=0$	O,L	O: center, L: singular line $x=-1$	
$\mu_2<-1$	$\mu_1>0$	O,E	O: source	E: sink
	$\mu_1=0$		O: center	E: center

Lemma 3.2. *For each $(\mu_1,\mu_2)\in[0,+\infty)\times\mathbb{R}$, the location and topological structure of equilibria at infinity of system* (1.9) *are listed in* Table 2*, and the dynamics of system* (1.9) *near infinity in the Poincaré disc are shown in Figure 3.*

TABLE 2. Location and topological structure of equilibria at infinity of system (1.9)

$(\mu_1,\mu_2)\in[0,+\infty)\times\mathbb{R}$		Number	Location	Topological structure
$\mu_2>0$		3	I_M^+: $y=\frac{1}{\sqrt{\mu_2}}x$, $x\to+\infty$ I_M^-: $y=\frac{1}{\sqrt{\mu_2}}x$, $x\to-\infty$	I_M: stable node
			I_N^+: $y=-\frac{1}{\sqrt{\mu_2}}x$, $x\to+\infty$ I_N^-: $y=-\frac{1}{\sqrt{\mu_2}}x$, $x\to-\infty$	I_N: unstable node
			I_P^+: $(0,+\infty)$ I_P^-: $(0,-\infty)$	I_P: saddle
$-1<\mu_2\le0$		1	I_P^+: $(0,+\infty)$ I_P^-: $(0,-\infty)$	I_P: stable node
$\mu_2=-1$	$\mu_1>0$	1	I_P^+: $(0,+\infty)$ I_P^-: $(0,-\infty)$	I_P: consist of one parabolic sector and two hyperbolic sectors
	$\mu_1=0$		I_P^+: $(0,+\infty)$ I_P^-: $(0,-\infty)$	I_P: consist of one singular line
$\mu_2<-1$		1	I_P^+: $(0,+\infty)$ I_P^-: $(0,-\infty)$	I_P: saddle

beginproof By the Poincaré transformation $x=1/z$, $y=u/z$, system (1.9) transforms into

$$\begin{aligned}\dot{u}&=1+z-\mu_2u^2-\mu_1uz+u^2z,\\ \dot{z}&=-\mu_1z^2-\mu_2uz+uz^2.\end{aligned}\tag{3.1}$$

We focus on studying equilibria of system (3.1) on the u-axis, reflecting the dynamics of system (1.9) at infinity except for equilibria at infinity on the y-axis, see [36]. Similarly, using another Poincaré transformation $x=v/z$, $y=1/z$, system (1.9) transforms into

$$\begin{aligned}\dot{v}&=\mu_2v-z+\mu_1vz-v^2z-v^3,\\ \dot{z}&=-vz^2-v^2z.\end{aligned}\tag{3.2}$$

It is easy to check that the origin $P:=(0,0)$ is an equilibrium of system (3.2). The qualitative properties of P reflect the dynamics of equilibria at infinity of system (1.9) on the y-axis, see [36]. In the following analysis, we analyze the qualitative properties of equilibria of system (3.1) on the u-axis and P of system (3.2). For system (3.1), we study it by two distinct cases.

Firstly, consider the case $\mu_2\le0$ in system (3.1). Clearly, system (3.1) has no equilibria on the u-axis.

Secondly, consider the case $\mu_2>0$ in system (3.1). It is easy to compute that system (3.1) has two equilibria $M:=(1/\sqrt{\mu_2},0)$ and $N:=(-1/\sqrt{\mu_2},0)$ on the u-axis. The eigenvalues of the

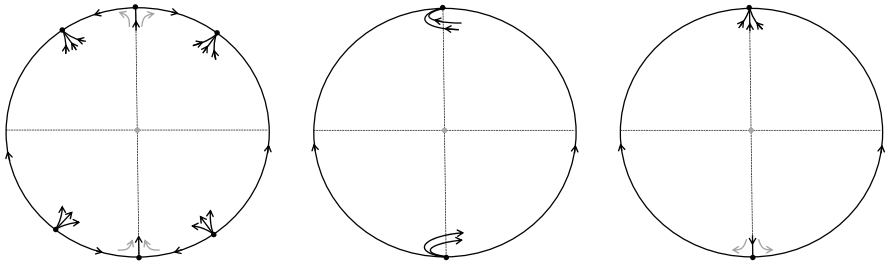

(a) $\mu_2 > 0$ (b) $-1 < \mu_2 \leq 0$ (c) $\mu_2 = -1$ and $\mu_1 > 0$

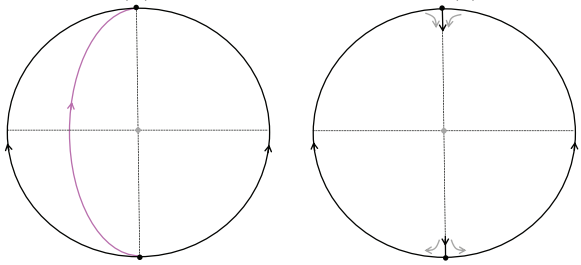

(d) $\mu_2 = -1$ and $\mu_1 = 0$ (e) $\mu_2 < -1$

FIGURE 3. Equilibrium points at infinity in the Poincaré disc of system (1.9) for $(\mu_1, \mu_2) \in [0, +\infty) \times \mathbb{R}$

linearization at M are $-2\sqrt{\mu_2}$ and $-\sqrt{\mu_2}$, whereas those at N are $2\sqrt{\mu_2}$ and $\sqrt{\mu_2}$. Therefore, M is a stable node and N is an unstable node, as shown in Figure 4(a).

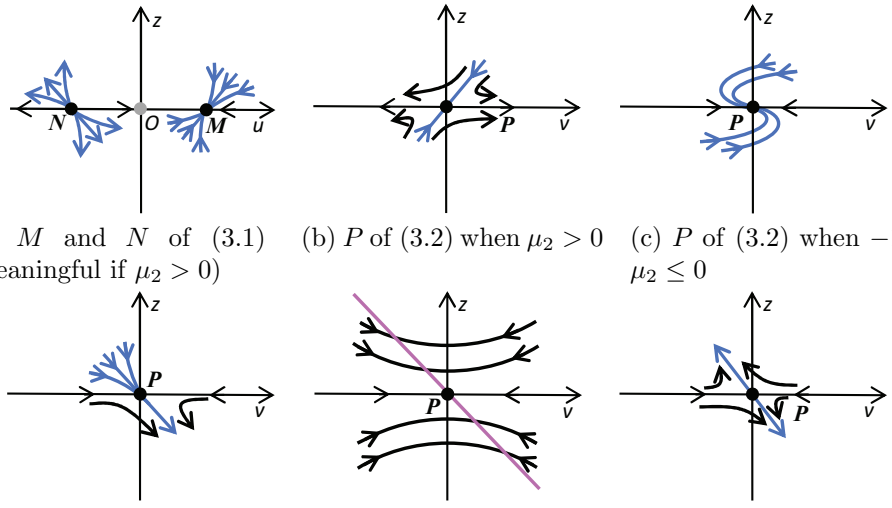

(a) M and N of (3.1) (meaningful if $\mu_2 > 0$) (b) P of (3.2) when $\mu_2 > 0$ (c) P of (3.2) when $-1 < \mu_2 \leq 0$

(d) P of (3.2) when $\mu_2 = -1$ and $\mu_1 > 0$ (e) P of (3.2) when $\mu_2 = -1$ and $\mu_1 = 0$ (f) P of system (3.2) when $\mu_2 < -1$

FIGURE 4. Qualitative properties of equilibria M, N and P

Finally, we study P of system (3.2). The eigenvalues of the linearization at P are μ_2 and 0. We first consider $\mu_2 = 0$ in system (3.2). Let $\overline{z} = -z + \mu_1 vz - v^2 z - v^3$, system (3.2) can be changed into

$$\dot{v} = \overline{z},$$
$$\dot{\overline{z}} = -v^5(1 + O(v)) - 4v^2\overline{z}(1 + O(v)) + \overline{z}^2 p(v, \overline{z}),$$

implying that P of system (3.2) is stable node by [36, Theorem 7.3], where $p(v,\overline{z})$ is analytic in a neighborhood of P. Second, consider $\mu_2 \neq 0$ in system (3.2). A simple calculation for $\mu_2 v - z + \mu_1 vz - v^2 z - v^3 = 0$ by the implicit function theorem leads to the solution

$$v = \frac{1}{\mu_2} z - \frac{\mu_1}{\mu_2^2} z^2 + O(z^3). \tag{3.3}$$

Substituting (3.3) into the second equation of system (3.2), we obtain

$$\dot{z} = -\frac{1+\mu_2}{\mu_2^2} z^3 + \frac{2\mu_1 + \mu_1\mu_2}{\mu_2^3} z^4 + O(z^5).$$

It follows from [36, Theorem 7.1] that P is a saddle as $\mu_2 > 0$ or $\mu_2 < -1$, a stable node as $-1 < \mu_2 < 0$, or a saddle-node as $\mu_2 = -1$ and $\mu_1 > 0$. For $\mu_2 = -1$ and $\mu_1 = 0$, system (3.2) is simplified into

$$\begin{aligned} \dot{v} &= -(v^2+1)(v+z), \\ \dot{z} &= -vz(v+z). \end{aligned} \tag{3.4}$$

Clearly, system (3.4) has one singular line $v = -z$ and the qualitative properties P of system (3.2) are easily obtained. Thus, the qualitative properties of P of system (3.4) are completely classified, as displayed in Figure 4(b-f).

Let I_M^+ and I_M^- be respectively the corresponding equilibria at infinity of M on the right half and left half plane, and similarly I_N^+ and I_N^- for N. Let I_P^+ and I_P^- at infinity on the positive and negative y-axis. Then, Table 2 and Figure 3 follow.

Proof of Theorem 2.1. By Lemma 3.2, the pitchfork bifurcation curve at infinity P and the degenerate equilibrium bifurcation curve at infinity DE_1 follow. Moreover, by Chapter 14 of [35, p.305], system (1.9) admits no limit cycles. Indeed, this follows from the Dulac criterion by taking

$$B = \frac{1}{1-\mu_2 x}$$

in each simply connected component of the region, where $1 - \mu_2 x \neq 0$.

We discuss the case $\mu_1 = 0$. In this case, system (1.9) becomes

$$\begin{aligned} \dot{x} &= -y + \mu_2 xy, \\ \dot{y} &= x + x^2. \end{aligned} \tag{3.5}$$

The phase portraits of system (3.5) are symmetric with respect to the x-axis, since it is invariant under the transformation $(y,t) \to (-y,-t)$. By Lemma 3.1, the origin O is a center. If $\mu_2 \neq -1$, system (3.5) has another equilibrium $E = (-1,0)$.

Let $(\mu_1,\mu_2) \in P_2$. Then, by Lemma 3.1, system (3.5) has exactly two equilibria O and $E: (-1,0)$, where O is a center and E is a saddle. On the other hand, Lemma 3.2 gives the dynamical behaviors of system (3.5) near infinity in the Poincaré disc, as shown in Figure 3(b). Denote by W_E^{rs} and W_E^{ru} the right-hand stable and unstable manifolds of the saddle E, respectively. The symmetry of (3.5) implies that these two manifolds are symmetric with respect to the x-axis. In view of the absence of limit cycles, they cannot enter a bounded annular region surrounding the center O. Consequently, the stable manifold W_E^{rs} must connect to the unstable manifold W_E^{ru}, forming a homoclinic loop. Therefore, the global phase portrait in the Poincaré disc in P_2 is shown in Figure 1(e).

Next, let $(\mu_1,\mu_2) \in DE_{12}$. By Lemma 3.1, system (3.5) has the center O and the singular line $L: x = -1$. Furthermore, Lemma 3.2 shows the dynamical behaviors of system (3.5) near infinity in the Poincaré disc, as given in Figure 3(d). The symmetry with respect to the x-axis, together with the nonexistence of limit cycles, fixes the possible global connections. Consequently, for parameters in DE_{12}, the global phase portrait in the Poincaré disc is as shown in Figure 1(i).

We now turn to the case $(\mu_1,\mu_2) \in P_1$. Take two parameter values $(\tilde{\mu}_1,\mu_2)$ and $(\bar{\mu}_1,\mu_2)$ in P_1 with $\bar{\mu}_1 > \tilde{\mu}_1$. A direct computation gives

$$\det \begin{pmatrix} \tilde{\mu}_1 x - y + \mu_2 xy & x(1+x) \\ \bar{\mu}_1 x - y + \mu_2 xy & x(1+x) \end{pmatrix} = (\tilde{\mu}_1 - \bar{\mu}_1) x^2 (1+x) \leq 0$$

for

$$(x,y)\in\{(x,y):x\geq -1,\ y\in\mathbb{R}\}.$$

Thus, in this region, the vector field of system (1.9) is rotated clockwise with increasing μ_1 [36, Chapter 4]. Starting from the homoclinic loop obtained in P_2, increasing μ_1 from zero destroys the homoclinic loop of the saddle E. More precisely, the stable and unstable manifolds of E rotate clockwise, and the former loop breaks. Since periodic orbits are excluded by the Dulac criterion, the right-hand stable manifold W_E^{rs} cannot bound a separatrix cycle. It must therefore have O as its α-limit set. This determines the global phase portrait in the Poincaré disc in P_1, as shown in Figure 1(d).

The global phase portraits in the remaining five parameter regions can be obtained in the same way. □

3.2. **Equilibria of system** (1.10)**.** We give the qualitative properties of equilibria of system (1.10)

Lemma 3.3. *For each* $(a,b,c)\in\mathbb{R}^2\times[0,+\infty)$*, equilibria of system* (1.10) *and their qualitative properties are given in* Tables 3 and 4*, where*

$$E_0:=(0,0),\quad E_1:=(x_1,1+cx_1),\quad E_2:=(x_2,1+cx_2),$$
$$E_{12}:=\Big(\frac{2}{a+b-c},1+\frac{2c}{a+b-c}\Big),\quad E_3:=\Big(\frac{b}{1+ab+b^2},\frac{ab+b^2}{1+ab+b^2}\Big),$$

with

$$x_1:=\frac{c-a-b+\sqrt{(c-a-b)^2+4(1+bc)}}{2(1+bc)},$$
$$x_2:=\frac{c-a-b-\sqrt{(c-a-b)^2+4(1+bc)}}{2(1+bc)}.$$

Proof. The number of equilibria in system (1.10) is determined by the equations $x^2+ax+(bx-1)y=0$ and $x(1+cx-y)=0$. Clearly, E_0 must be an equilibrium of system (1.10). Additionally, other equilibria (x_*,y_*) must satisfy

$$(1+bc)x_*^2+(a+b-c)x_*-1=0 \text{ and } y_*=1+cx_*. \tag{3.6}$$

Therefore, system (1.10) has at most two equilibria when $bc=-1$ and at most three equilibria when $bc\neq -1$, see Tables 3 and 4. In what follows, we study the qualitative properties of equilibria of system (1.10).

The Jacobian matrix J_{E_0} of system (1.10) at E_0 satisfies $\det J_{E_0}=1$ and $\operatorname{tr}J_{E_0}=a$. Since $(\operatorname{tr}J_{E_0})^2-4\det J_{E_0}=a^2-4$, E_0 is an unstable node for $a\geq 2$, an unstable focus for $0<a<2$, a stable focus for $-2<a<0$, a stable node for $a\leq -2$. For $a=0$, we divide into three cases $b=c=0$, $b=c\neq 0$ and $b\neq c$ to do test for center or focus. When $a=b=c=0$, system (1.10) is simplified as

$$\begin{aligned}\dot{x}&=-y+x^2\\ \dot{y}&=x-xy.\end{aligned} \tag{3.7}$$

Clearly, E_0 is a center as $a=b=c=0$ because system (3.7) is invariant under the transformation $(x,t)\to(-x,-t)$. When $a=0$ and $b=c\neq 0$, system (1.10) becomes

$$\begin{aligned}\dot{x}&=-y+x^2+bxy\\ \dot{y}&=x+bx^2-xy.\end{aligned} \tag{3.8}$$

By [36, Theorem 5.2 p.98], we obtain $W_1=0$ and $W_2=-4b(1+b^2)^2$ in system (3.8) inferring that E_0 is a stable fine focus of order two as $a=0$ and $b=c>0$, or an unstable fine focus of order two as $a=0$ and $b=c<0$. When $a=0$ and $b\neq c$, by [36, Theorem 5.2 p.98] again, we get $W_1=b-c$ in system (1.10) inferring that E_0 is an unstable fine focus of order one as $a=0$ and $b>c$, or a stable fine focus of order one as $a=0$ and $b<c$. Therefore, the qualitative properties of E_0 are completely classified.

TABLE 3. Nmberic and qualitative properties of equilibria of system (1.10)

Possibilities of $(a,b,c)\in\mathbb{R}^2\times[0,+\infty)$			Equilibria	Type and Stability	
$c=0$	$b>0$	$a>0$	E_0, E_1, E_2	E_0: source	E_1, E_2: saddles
		$a=0$		E_0: unstable FO	
		$a<0$		E_0: sink	
	$b=0$	$a>0$		E_0: source	
		$a=0$		E_0: center	
		$a<0$		E_0: sink	
	$b<0$	$a>0$		E_0: source	
		$a=0$		E_0: stable FO	
		$a<0$		E_0: sink	
$c>0$	$b>c$	$a>0$	E_0, E_1, E_2	E_0: source	E_1, E_2: saddles
		$a=0$		E_0: unstable FO	
		$a<0$		E_0: sink	
	$b=c$	$a>0$		E_0: source	
		$a=0$		E_0: stable FT	
		$a<0$		E_0: sink	
	$-\frac{1}{c}<b<c$	$a>0$		E_0: source	
		$a=0$		E_0: stable FO	
		$a<0$		E_0: sink	
	$b=-\frac{1}{c}$	$a>c-b$	E_0, E_3	E_0: source, E_3: saddle	
		$a=c-b$	E_0	E_0: source	
		$0<a<c-b$	E_0, E_3	E_0: source	E_3: saddle
		$a=0$		E_0: stable FO	
		$a<0$		E_0: sink	
	$-c-\frac{1}{c}<b<-\frac{1}{c}$	$a>a_1$	E_0, E_1, E_2	E_0: source	E_1: saddle, E_2: source
		$a=a_1$	E_0, E_{12}		E_{12}: saddle-node
		$a_2<a<a_1$	E_0		
		$a=a_2$	E_0, E_{12}		E_{12}: saddle-node
		$0<a<a_2$	E_0, E_1, E_2		E_1: source, E_2: saddle
		$a=0$		E_0: stable FO	
		$a<0$		E_0: sink	
	$b=-c-\frac{1}{c}$	$a>4c+\frac{1}{c}$	E_0, E_1, E_2	E_0: source	E_1: saddle, E_2: source
		$a=4c+\frac{1}{c}$	E_0, E_{12}		E_{12}: saddle-node
		$\frac{1}{c}<a<4c+\frac{1}{c}$	E_0		
		$a=\frac{1}{c}$	E_0, E_{12}		E_{12}: cusp
		$0<a<\frac{1}{c}$	E_0, E_1, E_2		E_1: source, E_2: saddle
		$a=0$		E_0: stable FO	
		$a<0$		E_0: sink	

Denote FO as fine focus of order one and FT as fine focus of order two.

Denote $a_1:=c-b+2\sqrt{-bc-1}$ and $a_2:=c-b-2\sqrt{-bc-1}$.

At the equilibrium (x_*,y_*), the linearization $J_{(x_*,y_*)}$ satisfies

$$\begin{aligned}\det J_{(x_*,y_*)}&=x_*\big[(c-a-b)-2x_*(1+bc)\big],\\ \operatorname{tr} J_{(x_*,y_*)}&=a+b+x_*(1+bc).\end{aligned}\tag{3.9}$$

We next analyze the qualitative properties of E_1, E_2, E_{12}, and E_3 in turn.

TABLE 4. Continuation of Table 3

<table>
<tr><th colspan="3">Possibilities of $(a,b,c)\in\mathbb{R}^2\times[0,+\infty)$</th><th>Equilibria</th><th colspan="3">Type and Stability</th></tr>
<tr><td rowspan="10">$c>0$</td><td rowspan="10">$b<-c-\frac{1}{c}$</td><td>$a>a_1$</td><td>E_0, E_1, E_2</td><td rowspan="5">E_0: source</td><td colspan="2">E_1: saddle, E_2: source</td></tr>
<tr><td>$a=a_1$</td><td>E_0, E_{12}</td><td colspan="2">E_{12}: saddle-node</td></tr>
<tr><td>$a_2<a<a_1$</td><td>E_0</td><td colspan="2" rowspan="2"></td></tr>
<tr><td>$a=a_2$</td><td>E_0, E_{12}</td></tr>
<tr><td>$\frac{1}{c}\le a<a_2$</td><td rowspan="5">E_0, E_1, E_2</td><td>E_{12}: saddle-node</td><td></td></tr>
<tr><td>$0<a<\frac{1}{c}$</td><td>E_1: sink</td><td rowspan="3">E_2: saddle</td></tr>
<tr><td>$a=0$</td><td>E_0: stable FO</td><td rowspan="2">E_1: source</td></tr>
<tr><td>$a<0$</td><td>E_0: sink</td></tr>
</table>

Firstly, we study E_1 and E_2. According to (3.6), we know that E_1 and E_2 exist if and only if $bc>-1$, or $bc<-1$ and $a>a_1:=c-b+2\sqrt{-bc-1}$, or $bc<-1$ and $a<a_2:=c-b-2\sqrt{-bc-1}$ (i.e., $\Delta>0$ of the first equation of (3.6)). By (3.9), we have

$$\det J_{E_1}=-\frac{c-a-b+\sqrt{(c-a-b)^2+4(1+bc)}}{2(1+bc)}\sqrt{(c-a-b)^2+4(1+bc)},$$
$$\det J_{E_2}=\frac{c-a-b-\sqrt{(c-a-b)^2+4(1+bc)}}{2(1+bc)}\sqrt{(c-a-b)^2+4(1+bc)},$$
$$\operatorname{tr} J_{E_1}=\frac{c+a+b+\sqrt{(c-a-b)^2+4(1+bc)}}{2},$$
$$\operatorname{tr} J_{E_2}=\frac{c+a+b-\sqrt{(c-a-b)^2+4(1+bc)}}{2}.$$

Thus, E_1 and E_2 are saddles as $bc>-1$, because $\det J_{E_1}<0$ and $\det J_{E_2}<0$. Additionally, E_1 is also a saddle as $bc<-1$ and $a>a_1$, and E_2 is also a saddle as $bc<-1$ and $a<a_2$. However, when $bc<-1$ and $a<a_2$, implying $\det J_{E_1}>0$, we need to further determine the sign of $\operatorname{tr} J_{E_1}$ by three cases $-c-1/c<b<-1/c$, $b=-c-1/c$, and $b<-c-1/c$. Consider the first case $-c-1/c<b<-1/c$, where $-c-1/c<b$ is equivalent to $a_2>-b-c$. Then we easily obtain $\operatorname{tr} J_{E_1}>0$. This is because it is clear that $\operatorname{tr} J_{E_1}>0$ when $-b-c\le a<a_2$ and we can compute $\operatorname{tr} J_{E_1}>0$ by

$$\operatorname{tr} J_{E_1}\cdot 2\left(c+a+b-\sqrt{(c-a-b)^2+4(1+bc)}\right)=4(ac-1) \tag{3.10}$$

when $a<-b-c$. Equation (3.10) is negative because $ac<-bc-c^2<(c+1/c)c-c^2=1$. Consider the second case $b=-c-1/c$, which is equivalent to $a_2=-b-c$, and then we also readily derive $\operatorname{tr} J_{E_1}>0$. This is because when $a<a_2=-b-c$, equation (3.10) is still negative since $ac<-bc-c^2=(c+1/c)c-c^2=1$. Consider the third case $b<-c-1/c$, which is equivalent to $a_2<-b-c$, and then when $a<a_2$ we easily obtain that $\operatorname{tr} J_{E_1}<0$ if $a>1/c$, $\operatorname{tr} J_{E_1}=0$ if $a=1/c$, and $\operatorname{tr} J_{E_1}>0$ if $a<1/c$. This is because $a_2>1/c$ when $b<-c-1/c$. When $b<-c-1/c$ and $a=1/c$, E_1 is a stable focus. Based on the analysis of the three cases described above, we conclude that when $bc<-1$ and $a<a_2$, E_1 is a source when $-c-1/c\le b<-1/c$, or $b<-c-1/c$ and $a<1/c$, and a sink when $b<-c-1/c$ and $a\ge 1/c$. Therefore, the qualitative properties of E_1 are completely classified. In the remaining cases concerning E_2, when $bc<-1$ and $a>a_1$, implying $\det J_{E_2}>0$, E_2 is a source because

$$\operatorname{tr} J_{E_2}\cdot 2\left(c+a+b+\sqrt{(c-a-b)^2+4(1+bc)}\right)=4(ac-1)>0. \tag{3.11}$$

(3.11) holds since $ac>c^2-bc+2c\sqrt{-bc-1}>c^2+1+2c\sqrt{-bc-1}$. Thus, the qualitative properties of E_2 are completely classified.

Secondly, we study E_{12}. From (3.6), we know that E_{12} exists if and only if $bc<-1$ and $|a+b-c|=\sqrt{-4(1+bc)}$ (i.e., $\Delta=0$ of the first equation of (3.6)). According to (3.9), we get $\det J_{E_{12}}=0$ and $\operatorname{tr} J_{E_{12}}=(a+b+c)/2$. We further subdivide the discussion into two cases

$a+b+c=0$ and $a+b+c\neq 0$. When $a+b+c=0$, we obtain $a=1/c$, $b=-1/c-c$, $E_{12}=(-1/c,0)$, and system (1.10) becomes

$$\begin{aligned}\dot{x}&=-cx+y+c^2x^2-(c+c^3)xy\\ \dot{y}&=-c^2x+cy+c^3x^2-c^2xy\end{aligned}\tag{3.12}$$

by the transformation $(x,t)\to(x-1/c,c^2t)$. Using the transformation $(x,y)\to(x,\widetilde{y}+cx)$, system (3.12) is changed into

$$\begin{aligned}\dot{x}&=\widetilde{y}-c^4x^2-(c+c^3)x\widetilde{y}\\ \dot{\widetilde{y}}&=c^4x(\widetilde{y}+cx).\end{aligned}\tag{3.13}$$

Let $\widetilde{\widetilde{y}}=\widetilde{y}-c^4x^2-(c+c^3)x\widetilde{y}$, system (3.13) can be further changed into

$$\begin{aligned}\dot{x}&=\widetilde{\widetilde{y}}\\ \dot{\widetilde{\widetilde{y}}}&=c^5x^2(1+O(x))-c^4x\widetilde{\widetilde{y}}(1+O(x))+\widetilde{\widetilde{y}}^2p(x,\widetilde{\widetilde{y}}),\end{aligned}\tag{3.14}$$

implying that the origin of system (3.14) is a cusp by [36, Theorem 7.3,p.132], where $p(x,\widetilde{\widetilde{y}})$ is analytic in a neighborhood of the origin. So is E_{12}. When $a+b+c\neq 0$, we easily obtain that E_{12} is a saddle-node by Theorem 7.1 of [36, p.114]. Thus, the qualitative properties of E_{12} are completely classified.

Finally, study E_3. By (3.6), we know that E_3 exists if and only if $bc=-1$ and $a+b-c\neq 0$. By (3.9), we have $\det J_{E_3}=-1$. Therefore, E_3 is a saddle. The proof is complete. □

To study the global dynamics of system (1.10), we perform a study at infinity.

Lemma 3.4. *For each $(a,b,c)\in\mathbb{R}^2\times[0,+\infty)$, the location and topological structure of equilibria at infinity of system* (1.10) *are illustrated in* Table 5*, and the dynamics of system* (1.10) *near infinity in the Poincaré disc are shown in Figure 5.*

Proof. Using the Poincaré transformation $x=1/z, y=u/z$, system (1.10) becomes

$$\begin{aligned}\dot{u}&=c-2u+z-bu^2-auz+u^2z\\ \dot{z}&=-z-az^2-buz+uz^2.\end{aligned}\tag{3.15}$$

We focus on studying equilibria of system (3.15) on the u-axis, reflecting the dynamics of system (1.10) at infinity except for equilibria at infinity on the y-axis, see [36]. At the equilibrium $(u_*,0)$ of system (3.15), the linearization $J_{(u_*,0)}$ satisfies

$$\begin{aligned}&\det J_{(u_*,0)}=2(1+bu)^2,\quad \operatorname{tr}J_{(u_*,0)}=-3(1+bu),\\ &\triangle_{(u_*,0)}:=(\operatorname{tr}J_{(u_*,0)})^2-4\det J_{(u_*,0)}=(1+bu)^2.\end{aligned}\tag{3.16}$$

Similarly, applying another Poincaré transformation $x=v/z$, $y=1/z$, system (1.10) becomes

$$\begin{aligned}\dot{v}&=bv-z+2v^2+avz-v^2z-cv^3\\ \dot{z}&=vz-vz^2-cv^2z.\end{aligned}\tag{3.17}$$

Evidently, the origin $Q:=(0,0)$ is an equilibrium of system (3.17). The qualitative properties of Q reflect the dynamics of equilibria at infinity of system (1.10) on the y-axis, see [36]. In what follows, we analyze the qualitative properties of equilibria of system (3.15) on the u-axis and Q of system (3.17). For system (3.15), we study it by four distinct cases.

Firstly, consider the case $b=0$ in system (3.15). It is easy to check that system (3.15) has a unique equilibrium $A:=(c/2,0)$. At the point A, it follows from (3.16) that $\det J_A=2>0$, $\operatorname{tr}J_A=-3<0$ and $\triangle_A=1>0$. It implies that A is a stable node, see Figure 6(a,b).

Secondly, consider the case $c>0$ and $b\in(-1/c,0)\cup(0,+\infty)$, or the case $c=0$ and $b\neq 0$ in system (3.15). It is easy to compute that system (3.15) has two equilibria $B:=((1+\sqrt{1+bc})/(-b),0)$ and $C:=((1-\sqrt{1+bc})/(-b),0)$, where $c>0$ or $c=0$. At the points B and C, it follows from (3.16) that $\det J_B=\det J_C=2(1+bc)>0$, $\operatorname{tr}J_B=3\sqrt{1+bc}>0$, $\operatorname{tr}J_C=-3\sqrt{1+bc}<0$, and $\triangle_B=\triangle_C=1+bc>0$, where $c>0$ or $c=0$. It means that B is an unstable node and C is a stable node, see Figure 6(c-f).

TABLE 5. Location and topological structure of equilibria at infinity of system (1.10)

Possibilities of $(a,b,c)\in\mathbb{R}^2\times[0,+\infty)$		Number	Location	Topological structure
$c=0$	$b\neq 0$	3	I_B^+: $y=\frac{2}{-b}x$, $x\to+\infty$ I_B^-: $y=\frac{2}{-b}x$, $x\to-\infty$ I_C^+: $(+\infty,0)$ I_C^-: $(-\infty,0)$ I_Q^+: $(0,+\infty)$ I_Q^-: $(0,-\infty)$	I_B: unstable node I_C: stable node I_Q: saddle-node
	$b=0$	2	I_A^+: $(+\infty,0)$ I_A^-: $(-\infty,0)$ I_Q^+: $(0,+\infty)$ I_Q^-: $(0,-\infty)$	I_A: stable node I_Q: consist of one hyperbolic sector and one elliptic sector
$c>0$	$b>0$ or $-\frac{1}{c}<b<0$	3	I_B^+: $y=\frac{1+\sqrt{1+bc}}{-b}x$, $x\to+\infty$ I_B^-: $y=\frac{1+\sqrt{1+bc}}{-b}x$, $x\to-\infty$ I_C^+: $y=\frac{1-\sqrt{1+bc}}{-b}x$, $x\to+\infty$ I_C^-: $y=\frac{1-\sqrt{1+bc}}{-b}x$, $x\to-\infty$ I_Q^+: $(0,+\infty)$ I_Q^-: $(0,-\infty)$	I_B: unstable node I_C: stable node I_Q: saddle-node
	$b=0$	2	I_A^+: $y=\frac{c}{2}x$, $x\to+\infty$ I_A^-: $y=\frac{c}{2}x$, $x\to-\infty$ I_Q^+: $(0,+\infty)$ I_Q^-: $(0,-\infty)$	I_A: stable node I_Q: consist of one hyperbolic sector and one elliptic sector
	$b=-\frac{1}{c}$, $a\neq c-b$	2	I_D^+: $y=cx$, $x\to+\infty$ I_D^-: $y=cx$, $x\to-\infty$ I_Q^+: $(0,+\infty)$ I_Q^-: $(0,-\infty)$	I_D: one hyperbolic sector and one elliptic sector I_Q: saddle-node
	$b=-\frac{1}{c}$, $a=c-b$			I_D: two hyperbolic sectors I_Q: saddle-node
	$b<-\frac{1}{c}$	1	I_Q^+: $(0,+\infty)$ I_Q^-: $(0,-\infty)$	I_Q: saddle-node

Thirdly, consider the case $c>0$ and $b=-1/c$ in system (3.15). It is clear that system (3.15) has a unique equilibrium $D:=(-1/b,0)$. By $u\to u-1/b$, system (3.15) is changed into

$$\begin{aligned}\dot{u}&=\frac{1+ab+b^2}{b^2}z-bu^2-(a+\frac{2}{b})uz+u^2z\\ \dot{z}&=(-a-\frac{1}{b})z^2-buz+uz^2,\end{aligned}\tag{3.18}$$

implying that D of system (3.15) becomes the origin of system (3.18). We now turn to study the origin of system (3.18) by two cases $1+ab+b^2\neq 0$ and $1+ab+b^2=0$, i.e., $a\neq-(b^2+1)/b$ and $a=-(b^2+1)/b$.

Consider the case $a\neq-(b^2+1)/b$ in system (3.18). Notice that the Jacobian matrix at the origin of system (3.18) is a nilpotent matrix. By $t\to b^2t/(1+ab+b^2)$, system (3.18) can be

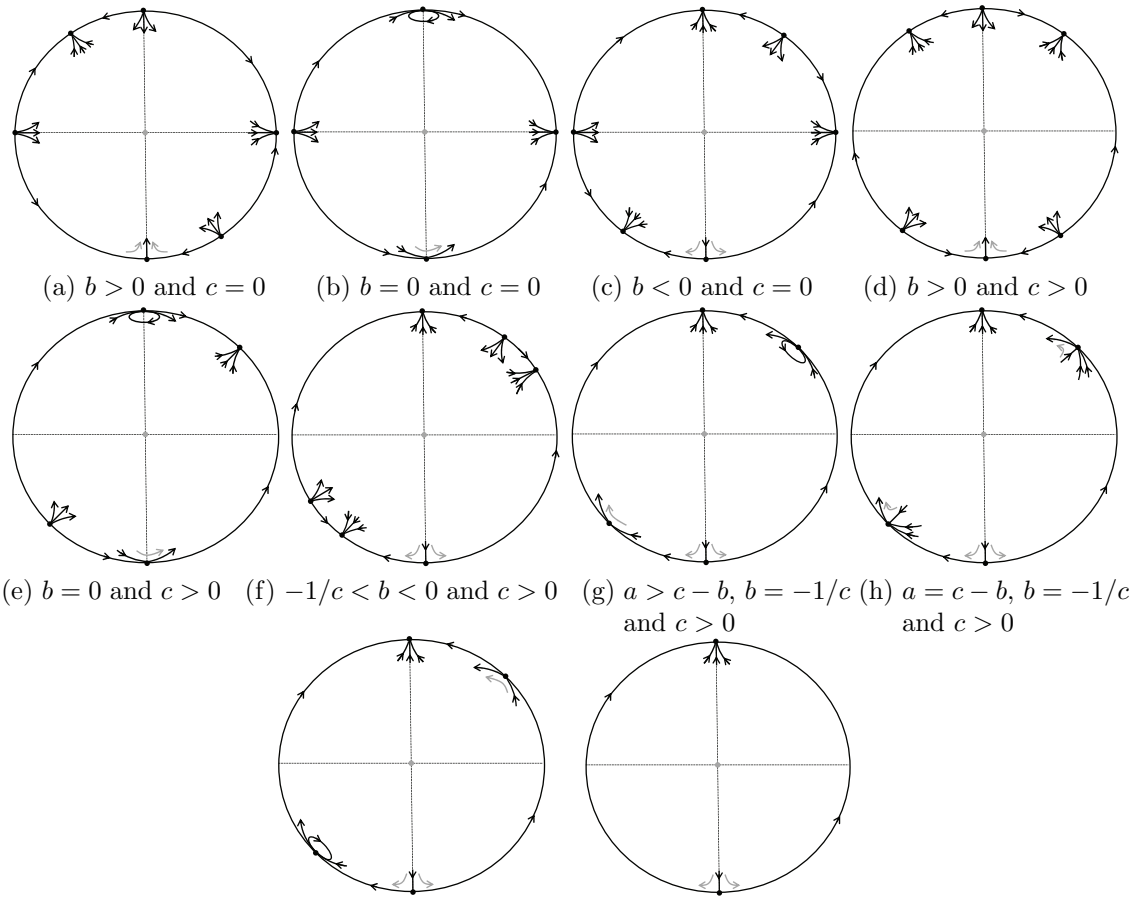

(a) $b>0$ and $c=0$ (b) $b=0$ and $c=0$ (c) $b<0$ and $c=0$ (d) $b>0$ and $c>0$

(e) $b=0$ and $c>0$ (f) $-1/c<b<0$ and $c>0$ (g) $a>c-b$, $b=-1/c$ and $c>0$ (h) $a=c-b$, $b=-1/c$ and $c>0$

(i) $a<c-b$, $b=-1/c$ and $c>0$ (j) $b<-1/c$ and $c>0$

FIGURE 5. Equilibrium points at infinity in the Poincaré disc of system (1.10) for $(a,b,c)\in\mathbb{R}^2\times[0,+\infty)$

written as

$$\begin{aligned}\dot{u}&=z-\frac{b^3}{1+ab+b^2}u^2-\frac{b(ab+2)}{1+ab+b^2}uz+\frac{b^2}{1+ab+b^2}u^2z\\ \dot{z}&=-\frac{b(ab+1)}{1+ab+b^2}z^2-\frac{b^3}{1+ab+b^2}uz+\frac{b^2}{1+ab+b^2}uz^2.\end{aligned}\tag{3.19}$$

Letting

$$\widehat{z}=z-\frac{b^3}{1+ab+b^2}u^2-\frac{b(ab+2)}{1+ab+b^2}uz+\frac{b^2}{1+ab+b^2}u^2z,$$

system (3.19) can be rewritten as

$$\begin{aligned}\dot{u}&=\widehat{z},\\ \dot{\widehat{z}}&=-\frac{b^6}{(1+ab+b^2)^2}u^3(1+O(u))-\frac{3b^3}{1+ab+b^2}u\widehat{z}(1+O(u))+\widehat{z}^2p(u,\widehat{z}),\end{aligned}\tag{3.20}$$

where $p(u,\widehat{z})$ is analytic in a neighborhood of the origin of system (3.20). According to [36, Theorem 7.2, p.132], it follows that the origin of system (3.20) consists of a hyperbolic sector and an elliptic sector. So is D of system (3.15). See Figure 6(g,i).

Consider the case $a=-(b^2+1)/b$ in system (3.18). System (3.18) is simplified as

$$\begin{aligned}\dot{u}&=-bu^2-(-b+\frac{1}{b})uz+u^2z\\ \dot{z}&=bz^2-buz+uz^2.\end{aligned}\tag{3.21}$$

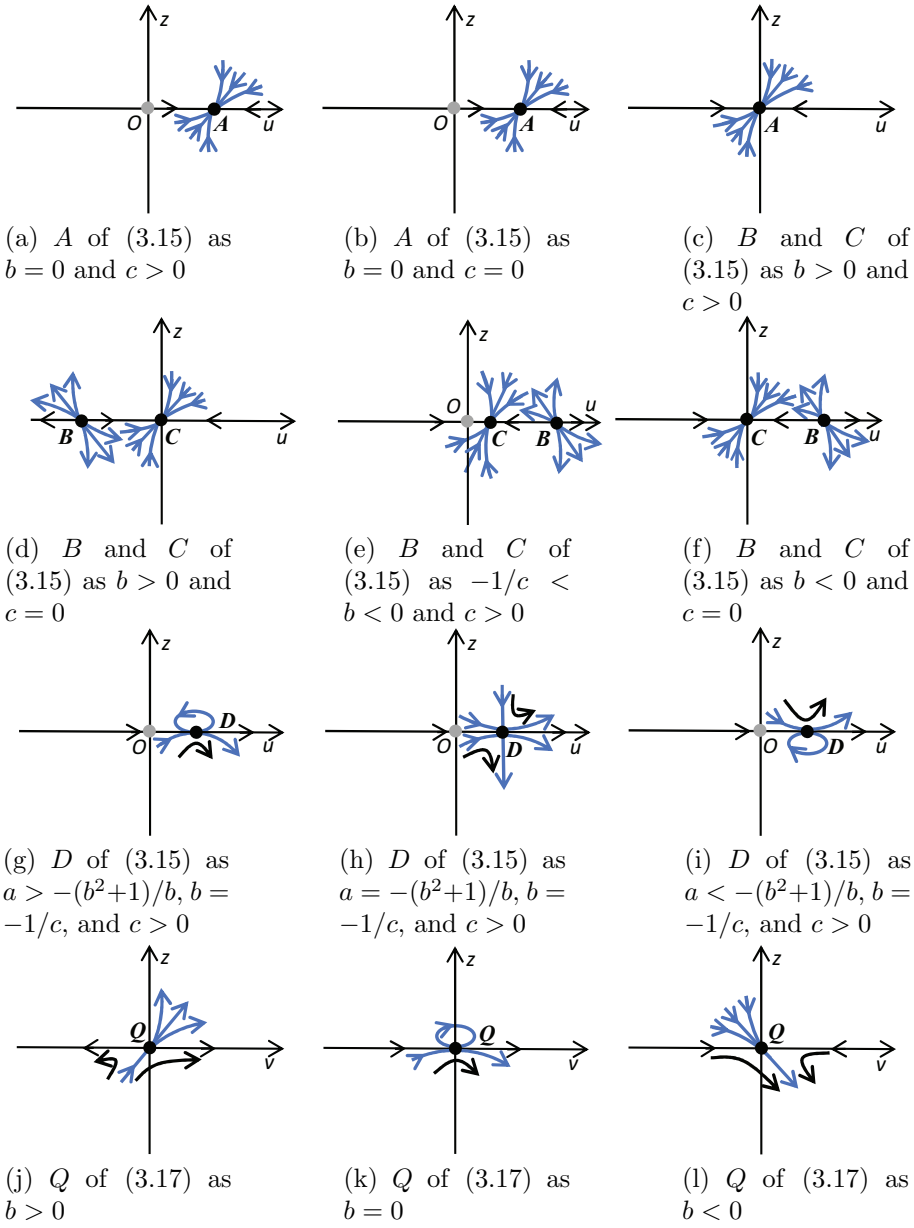

(a) A of (3.15) as $b = 0$ and $c > 0$

(b) A of (3.15) as $b = 0$ and $c = 0$

(c) B and C of (3.15) as $b > 0$ and $c > 0$

(d) B and C of (3.15) as $b > 0$ and $c = 0$

(e) B and C of (3.15) as $-1/c < b < 0$ and $c > 0$

(f) B and C of (3.15) as $b < 0$ and $c = 0$

(g) D of (3.15) as $a > -(b^2+1)/b$, $b = -1/c$, and $c > 0$

(h) D of (3.15) as $a = -(b^2+1)/b$, $b = -1/c$, and $c > 0$

(i) D of (3.15) as $a < -(b^2+1)/b$, $b = -1/c$, and $c > 0$

(j) Q of (3.17) as $b > 0$

(k) Q of (3.17) as $b = 0$

(l) Q of (3.17) as $b < 0$

FIGURE 6. Qualitative properties of equilibria A, B, C, D and Q

Clearly, the origin of system (3.21) is a degenerate equilibrium. Therefore, we shall adopt the method of normal sectors to study such an equilibrium, see [36, Chapter 2]. By polar coordinate transformation $u = r\cos\theta$ and $z = r\sin\theta$, system (3.21) can be written as the following polar form

$$\frac{1}{r}\frac{dr}{d\theta} = \frac{H(\theta) + \widetilde{H}(\theta, r)}{G(\theta) + \widetilde{G}(\theta, r)},$$

where

$$\begin{aligned} G(\theta) &= \frac{1}{b}\cos\theta\sin^2\theta, \\ H(\theta) &= b\sin^3\theta - b\cos^3\theta - b\cos\theta\sin^2\theta + (b - \frac{1}{b})\cos^2\theta\sin\theta. \end{aligned} \tag{3.22}$$

We know that $G(\theta) = 0$ is a necessary condition for $\theta = \theta_0$ to be an exceptional direction and there is no orbit connecting the equilibrium along other directions except the exceptional direction $\theta = \theta_0$, see [36, Chapter 2]. By (3.22), $G(\theta) = 0$ has the following four real roots

$$\theta_1 = 0, \quad \theta_2 = \frac{\pi}{2}, \quad \theta_3 = \pi, \quad \theta_4 = \frac{3\pi}{2}$$

for $\theta \in [0, 2\pi)$. We can easily check that

$$H(\theta_1) = H(\theta_4) = -b > 0, \quad H(\theta_2) = H(\theta_3) = b < 0.$$

Further, we can compute that

$$G''(\theta_1)H(\theta_1) = G''(\theta_3)H(\theta_3) = -2 < 0,$$
$$G'(\theta_2)H(\theta_2) = G'(\theta_4)H(\theta_4) = -1 < 0.$$

According to [36, Theorem 3.6 (resp. 3.4), Chapter 2], it follows that there is exactly one orbit approaching the origin of system (3.21) along the directions $\theta = \theta_2$ (resp. θ_4) as $t \to +\infty$ (resp. $-\infty$), and there are infinitely many orbits approaching the origin of system (3.21) along the direction $\theta = \theta_1$ (resp. θ_3) as $t \to -\infty$ (resp. $+\infty$). So is D of system (3.15). See Figure 6(h).

Fourthly, consider the case $c > 0$ and $b \in (-\infty, -1/c)$ in system (3.15). Evidently, system (3.15) has no equilibria on the u-axis.

Finally, we study Q system (3.17). The eigenvalues of the linearization at Q are b and 0. If $b = 0$, then letting $\widetilde{z} = -z + 2v^2 + avz - v^2z - cv^3$ system (3.17) can be changed into

$$\begin{aligned} \dot{v} &= \widetilde{z} \\ \dot{\widetilde{z}} &= -2v^3(1 + O(v)) + 5v\widetilde{z}(1 + O(v)) + \widetilde{z}^2 p(v, \widetilde{z}), \end{aligned} \tag{3.23}$$

where $p(v, \widetilde{z})$ is analytic in a neighborhood of Q. It follows from [36, Theorem 7.2 , p.132] that Q consists of a hyperbolic sector and an elliptic sector as $b = 0$, see Figure 6(k). If $b \neq 0$, then we easily obtain that Q is a saddle-node by [36, Theorem 7.1, p.114], see Figure 6(j,l).

Let I_A^+ and I_A^- be respectively the corresponding equilibria at infinity of A on the right half and left half plane, and similarly for B, C and D. Let I_Q^+ and I_Q^- at infinity on the positive and negative y-axis. Then, Table 5 and Figure 5 follow. The proof is complete. □

3.3. **Proof of Theorem 2.2.** Let $W_{E_1}^{ls}$ denote the stable manifold of the left-hand side of saddle E_1 and similarly for $W_{E_1}^{lu}$, $W_{E_2}^{rs}$ and $W_{E_2}^{ru}$. Before proving Theorem 2.2, we summarize six results obtained for system (1.10) with $c = 0$.

(I) By Lemma 3.3, system (1.10) with $c = 0$ has three equilibria E_0, E_1 and E_2, where E_1 and E_2 are always saddles on the line $y = 1$, with E_2 positioned to the left of E_1.

(II) By (I) and the vector field $\dot{y} = x(1 - y)$, there exists a heteroclinic connection from E_1 to E_2, i.e., $W_{E_1}^{lu}$ connects $W_{E_2}^{rs}$.

(III) By II and the index theory of [36, Chapter 4], the limit cycle of system (1.10) with $c = 0$ only surrounds E_0 if it exists.

(IV) By the theory of rotated vector fields [14, 36], the manifolds $W_{E_1}^{ls}$ and $W_{E_2}^{ru}$ rotate clockwise as a increases with b fixed.

(V) According to [35, Theorem 16.1], system (1.10) with $c = 0$ has a center when $a = b = 0$ and has no limit cycle when $a = 0$ and $b \neq 0$.

(VI) By [35, Theorem 15.4], if system (1.10) with $c = 0$ has a limit cycle, then it has at most one.

Proof of Theorem 2.2. For $(a, b, c) \in DE_{22}$, system (1.10) becomes

$$\begin{aligned} \dot{x} &= -y + x^2, \\ \dot{y} &= x - xy, \end{aligned} \tag{3.24}$$

whose phase portrait is symmetric with respect to the y-axis. By Lemma 3.3, system (3.24) has three equilibria E_0, E_1 and E_2, where E_0 is a center and E_1, E_2 are saddles. Moreover, Lemma 3.4 gives the behavior of system (3.24) near infinity in the Poincaré disc, as shown in Figure 5. We know that $W_{E_1}^{lu}$ connects $W_{E_2}^{rs}$ by (II). By (V) and the symmetry of system (3.24), the

stable manifold $W^{ls}_{E_1}$ of E_1 connects the unstable manifold $W^{ru}_{E_2}$ of E_2, forming a heteroclinic loop enclosing the center E_0. Therefore, for parameters in DE_{22}, the global phase portrait in the Poincaré disc is as depicted in Figure 2(k).

For $(a,b,c) \in DE_{21}$, we start from the heteroclinic loop obtained in DE_{22}, increasing a from zero destroys this loop. More precisely, by the theory of rotated vector fields, the manifolds $W^{ls}_{E_1}$ and $W^{ru}_{E_2}$ rotate clockwise as a increases, and hence the former heteroclinic connection breaks, according to (IV). We claim that no limit cycle exists. Otherwise, by the Poincaré-Bendixson annular region theorem, there exist at least two limit cycles, contradicting (VI). This proves the claim. Therefore, after the breaking of the heteroclinic loop, the stable manifold $W^{ls}_{E_1}$ must have E_0 as its α-limit set. This determines the global phase portrait in the Poincaré disc of DE_{21} shown in Figure 2(h).

For $(a,b,c) \in H_{11}$, Lemma 3.4 gives the behavior of system (1.10) with $c = 0$ near infinity in the Poincaré disc, as shown in Figure 5. By (V), no limit cycle exists. Similarly to the case DE_{22}, the global phase portrait in the Poincaré disc for H_{11} is as shown in Figure 2(b).

For $a < 0$ and $b > 0$, we start from the parameter region H_{11}, where the global separatrix configuration has already been obtained. Fix $b > 0$ and let a decrease. By (IV) together with the theory of rotated vector fields, the manifolds $W^{ls}_{E_1}$ and $W^{ru}_{E_2}$ rotate counterclockwise. Consequently, there exists a critical value $a = \varphi(b)$ such that $W^{ls}_{E_1}$ connects $W^{ru}_{E_2}$ when $a = \varphi(b)$. Hence a heteroclinic connection between E_1 and E_2 occurs on the curve $a = \varphi(b)$. Moreover, for each fixed $b > 0$, the monotonic rotation of the separatrices with respect to the parameter a implies the uniqueness of the critical value $a = \varphi(b)$. Furthermore, by the continuous dependence of solutions on parameters, the function $\varphi(b)$ is continuous.

For $a < \varphi(b)$, this heteroclinic connection is broken. In this case, the stable manifold $W^{ls}_{E_1}$ no longer connects with $W^{ru}_{E_2}$; instead, it tends to the infinite direction $(0, -\infty)$. Thus no annular region producing a limit cycle appears in this case.

For $\varphi(b) < a < 0$, the breaking of the above heteroclinic connection gives rise to an annular region. By the Poincaré-Bendixson annular region theorem, there exists at least one limit cycle. On the other hand, by (VI), there exists at most one limit cycle. Therefore, system (1.10) with $c = 0$ has a unique limit cycle in this case, which is unstable.

Accordingly, the global phase portraits in the Poincaré disc for S_2, HE_{11}, and S_3 are as shown in Figures 2(c), 2(j), and 2(d), respectively.

The remaining cases can be treated in the same way, and hence the corresponding proofs are omitted. Combining the above analysis, we obtain the heteroclinic bifurcation curve HE_1 and the global phase portraits in the corresponding parameter regions. □

Proof of Theorem 2.3. (i) By Lemma 3.3, the Hopf bifurcation surfaces H_2 and H_3 at E_0 and E_1, respectively, are obtained.

(ii) By Lemma 3.3, we obtain that the trace at E_0 is a, and the first focal value on $a = 0$ is $W_1 = b - c$. When $a = 0$ and $b = c > 0$, we have

$$W_1 = 0, \quad W_2 = -4b(1 + b^2)^2 < 0.$$

Hence, by [18, Chapter 8], system (1.10) exhibits a Bautin bifurcation at E_0 when $a = 0$ and $b = c > 0$, which gives the bifurcation curve B.

(iii) By Lemma 3.3, the equilibria E_1 and E_2 coalesce into the saddle-node E_{12} when $bc < -1$, $\Delta = 0$ and $a + b + c \neq 0$. Near such a parameter value, these two equilibria exist for $\Delta > 0$ and disappear for $\Delta < 0$. Hence, system (1.10) exhibits a saddle-node bifurcation on the surface SN.

(iv) By Lemma 3.3, we know that E_{12} is a nondegenerate cusp on BT. For each fixed $c > 0$, the parameters a and b provide a nondegenerate unfolding. Hence, by [18, Chapter 8], the Bogdanov–Takens bifurcation curve BT is obtained. □

Acknowledgments. This work is supported by the National Natural Science Foundation of China (No. 12501201).

References

[1] J. C. Artés, H. Chen, L .M. Ferrer, M. Jia; Quadratic vector fields in class I, *Dynam. Syst.*, **40**(2025), 191-222.

[2] J. C. Artés, J. Llibre, A. C. Rezende; *Structurally Unstable Quadratic Vector Fields of Codimension One*, Birkhäuser, Cham, 2018.

[3] X. Cen, H. Chen, Z. Feng, R. Zhang; A necessary and sufficient condition for general Rayleigh–Liénard system with an elementary center, *J. Nonlinear Sci.*, 36(2026) 50, 1–18.

[4] H. Chen, Z. Feng, M. Jia, Y. Meng; Maximum number of limit cycles of the piecewise linear Liénard system with three zones, *J. Lond. Math. Soc.*, 113(2026) e70430, 1–56.

[5] L. S. Chen, M. S. Wang; The relative position and number of limit cycles of a quadratic differential system, *Acta Math. Sinica*, **22**(1979), 751-758.

[6] S.-N. Chow, C. Li, D. Wang; *Normal Forms And Bifurcation of Planar Vector Fields*, Cambridge University Press, Cambridge, New York, 2007.

[7] W. A. Coppel; A survey of quadratic systems, *J. Differential Equations*, **2**(1966), 293-304.

[8] W. A. Coppel; Some quadratic systems with at most one limit cycle, *Dynamics Reported*, **2**(1989), 61-88.

[9] W. A. Coppel; A new class of quadratic systems, *J. Differential Equations*, **92**(1991), 360-372.

[10] F. Dumortier, J. Llibre, J. C. Artés; *Qualitative Theory of Planar Differential Systems*, Springer-Verlag, Berlin Heidelberg, 2006.

[11] A. Ferragut, J. D. García-Saldaña, C. Valls; Phase portraits of Abel quadratic differential systems of second kind with symmetries. *Dynam. Syst.*, 34(2019), 301-333.

[12] A. Ferragut, C. Valls; Phase portraits of Abel quadratic differential systems of the second kind, *Dynam. Syst.*, **33**(2018), 581-601.

[13] A. Gasull, H. Giacomini, S. Pérez-González, J. Torregrosa; A proof of Perko's conjectures for the Bogdanov-Takens system, *J. Differential Equations*, **255**(2013), 2655-2671.

[14] M. Han; Global behavior of limit cycles in rotated vector fields, *J. Differential Equations*, **151**(1999), 20-35.

[15] D. Hilbert; Mathematical Problems, *Bull. Amer. Math. Soc.*, **8** (1902), 437–479.

[16] Yu. Ilyashenko; Centennial history of Hilbert's 16th problem, *Bull. Amer. Math. Soc.*, **39**(2002), 301-354.

[17] M. Jia, H. Chen, H. Chen; Bifurcation diagram and global phase portraits of a family of quadratic vector fields in Class I, *Qual. Theo. Dyn. Syst.*, **19**(2020), 64–1-22.

[18] Y. A. Kuznetsov; *Elements of Applied Bifurcation Theory*, 2nd ed., Springer-Verlag, New York, 1998.

[19] J. Li; Hilbert's 16th problem and bifurcations of planar polynomial vector fields, *Int. J. Bifur. Chaos*, **13**(2003), 47-106.

[20] C. Li, Z. Zhang; Remarks on 16th weak Hilbert problem for $n = 2$, *Nonlinearity*, **15**(2002), 1975-1992.

[21] A. Lins, W. de Melo, C. C. Pugh; On Liénard's equation, *Lecture Notes in Math.*, **597**(1977), 335-357.

[22] D. S. Malkus, J. A. Nohel, B. J. Plohr; Dynamics of shear flow of a non-Newtonian fluid, *J. Comput. Phys.*, **87**(1990), 464-487.

[23] D. S. Malkus, J. A. Nohel, B. J. Plohr; Analysis of new phenomena in shear flow of non-Newtonian fluids, *SIAM J. Appl. Math.*, **51**(1991), 899-929.

[24] J. A. Nohel, R. L. Pego; Nonlinear stability and asymptotic behavior of shearing motions of a non-Newtonian fluid, *SIAM J. Math. Anal.*, **24**(1993), 911-942.

[25] L. Perko; A global analysis of the Bogdanov-Takens system, *SIAM J. Appl. Math.*, **52**(1992), 1172-1192.

[26] L. Perko; *Differential Equations and Dynamical Systems*, 3rd ed., Texts in Applied Mathematics, Springer, New York, 2001.

[27] J. W. Reyn; Phase portraits of quadratic systems without finite critical points, *Nonlinear Anal.*, **27**(1996), 207-222.

[28] J. W. Reyn; Phase portraits of quadratic systems with finite multiplicity one, *Nonlinear Anal.*, **28**(1997), 755-778.

[29] J. W. Reyn; *Phase Portraits of Planar Quadratic Systems*, Mathematics and Its Applications **583**, Springer, New York, 2007.

[30] J. W. Reyn, R. E. Kooij; Phase portraits of non-degenerate quadratic systems with finite multiplicity two, Mathematics and Its Applications, *Differ. Equ. Dyn. Syst.*, **5**(1997), 355-414.

[31] R. Roussarie; *Bifurcation of Planar Vector Fields and Hilbert's Sixteenth Problem*, Progress in Mathematics, Birkhäuser, Basel, 1998.

[32] G. S. Rychkov; A complete investigation of the number of limit cycles of the equation $(b_{10}x + y)dy = \sum_{i+j=1}^{2} a_{ij}x^i y^j dx$, *Differ. Equ.*, **6**(1970) 2193-2199. (in Russian)

[33] S. L. Shi; A concrete example of the existence of four limit cycles for plane quadratic systems, *Sci. China Ser. A*, **11**(1979), 1051-1056.

[34] Y. Tang, W. Zhang; Generalized normal sectors and orbits in exceptional directions, *Nonlinearity*, **17**(2004), 1407-1426.

[35] Y. Ye; *Theory of Limit Cycles*, Transl. Math. Monogr., Amer. Math. Soc., Providence, RI, 1986.

[36] Z. Zhang, T. Ding, W. Huang, Z. Dong; *Qualitative Theory of Differential Equations*, Transl. Math. Monogr., Amer. Math. Soc., Providence, RI, 1992.

[37] X. Zhang, Q. Ye; Uniqueness of limit cycles of quadratic system $(\mathrm{III})_{m=0}$, *Chinese Sci. Bull.*, **42**(1997), 628-631.

[38] H. Zoladek; Quadratic systems with center and their perturbations, *J. Differential Equations*, **109**(1994), 223-273.

Man Jia
School of Mathematics and Statistics, Fuzhou University, Fuzhou, Fujian 350116, China
Email address: manjia@fzu.edu.cn